

Universitat de Lleida

Document downloaded from:

<http://hdl.handle.net/10459.1/60308>

The final publication is available at:

<https://doi.org/10.1016/j.solmat.2017.09.029>

Copyright

cc-by-nc-nd, (c) Elsevier, 2017



Està subjecte a una llicència de [Reconeixement-NoComercial-SenseObraDerivada 4.0 de Creative Commons](https://creativecommons.org/licenses/by-nc-nd/4.0/)

1 Thermomechanical testing under operating conditions of A516Gr70 2 used for CSP storage tanks 3

4 Cristina Prieto¹, Camila Barreneche², Mònica Martínez², Luisa F. Cabeza³, A. Inés Fernández^{2,*}
5

6 ¹Abengoa Research, C/ Energía Solar nº 1, Palmas Altas,41014-Sevilla

7 ² Department of Materials Science & Physical Chemistry, Universitat de Barcelona, Martí i Franqués 1,
8 Barcelona 08028, Spain.

9 ³ GREA Innovació Concurrent, INSPIRES Research Centre, Universitat de Lleida, Pere de Cabrera s/n,
10 25001, Lleida, Spain.

11 *Corresponding authors: ana_inesfernandez@ub.edu

12 Abstract

13 Thermal energy storage (TES) in molten salts is the storage dominating technology in solar
14 power applications today. In two-tank molten salt storage systems energy density ranges from
15 30 to 70 kWh/m³ are achievable. The salt material used is a binary system, composed of 60%
16 NaNO₃ and 40% KNO₃. In the 8 MWh_{th} pilot plant built and tested by Abengoa, the storage
17 tanks were made of steel A516Gr.70 using the Appendix M of code API 650 for their design. A
18 specific testing device was developed to evaluate thermo-mechanical properties, and a study
19 was conducted in order to evaluate tensile properties of A516Gr.70 specimens under operation
20 conditions for the hot tank at the pilot plant that is in contact with molten salts at 380 °C.
21 Results confirmed the outcomes of the work: the reduction of the yield limit, elongation before
22 fracture, and Young modulus at 380 °C after having been 5 minutes immersed in molten salts.
23 Moreover, after a creep-test simulating operating 7 days conditions during, an additional
24 reduction of the yield limit was measured.

25
26 Key-words: *thermomechanical properties, concentrated solar power (CSP), thermal energy*
27 *storage (TES), carbon steel, molten salts, thermal treatment*

28 1. Introduction

29 The global crisis of energy is one of the biggest challenges for the near future for researchers
30 and policy makers in order to achieve a sustainable solution that deal with this energy crisis [1-
31 2]. Solar energy is the highest power source of the world. Thereby, solar power technologies are
32 able to produce high amounts of sustainable power. Concentrated solar power (CSP) plants [3-
33 4] are systems able to concentrate a large amount of solar energy using different types of
34 collectors; several characteristics of solar power plants are described by Desideri et al. [5].

35 Nowadays, thermal energy storage (TES) is a promising technology to be applied as a
36 complement of CPS plants in order to reduce the gap between energy supply and energy
37 demand [6]. Therefore, TES systems are implemented in CSP plants successfully by producing
38 electricity several hours after sunrise [7]. Moreover, TES will help in making CSP much more
39 viable and feasible from the economic and technical point of view. But the proper selection of
40 materials has a great significance not only to deal with a proper performance of the plant but
41 also for the economic interest of TES units.

42 A516Gr.70 steel was used to manufacture the storage tanks in the pilot plant of nitrate molten
43 salts with 8 MWh_{th} built by Abengoa [8]. A516Gr.70 is the main used steel in commercial CSP
44 plants due to its high mechanical performance efficiency under stress and its relative low cost.
45 Mechanical design typically uses the yield strength as one of the main design parameters.
46 However, it is well known that the mechanical properties of steels as the yield strength or the
47 modulus of elasticity decrease with increasing temperature. In this study, this change is of
48 extremely importance because during operation of both storage tanks, the cold one is designed
49 to operate at 288 °C and the hot one at 388 °C. Moreover, the maximum service temperature is
50 the highest temperature at which the material can be used for an extended period without
51 significant problems [9]. For the majority of commercial carbon steels, this temperature ranges
52 from 270 to 360°C and only few grades of steel are certified to work at higher temperatures like
53 the operation conditions of the hot tank of molten salts storage systems. Prieto et al. [8]
54 previously reported a detailed description of the tanks design. Both tanks were built with steel
55 A516 and two grades with different grain size. Thus, grade 60 with the smallest grain size was
56 used for the tank cover and grade 70 for the rest of the tank. Parameters used for the design were
57 those of the Appendix M of code API 650, although it only gives the requirements for working
58 temperatures between 90 °C and 260 °C.

59 The study of the evolution of the mechanical properties with temperature may be performed
60 varying temperature with special testing devices adapted for such purpose, and following
61 international standards for testing [11]. Nevertheless, the working conditions of this material in
62 operation, which are the temperature (388 °C) and the environment (in contact with nitrate
63 molten salts), are not considered in any standard. For this purpose, a study was conducted in
64 order to evaluate tensile properties under operation conditions by testing in a device developed
65 at the University of Barcelona, where a series of mechanical experiments were performed with
66 A516 gr70 carbon steel specimens in contact with molten salts at 380 °C. Prior and after the
67 mechanical testing, a metallographic study was performed.

68

70 **2. Methods and materials**

71 **2.1. Materials**

75 The specimens for this study were obtained from a plate of the same carbon steel used in the
76 construction of the tanks at the Abengoa plant. Table 1 summarizes the main characteristics
77 collected from the CES Selector database for the reference ASTM A516 Grade 70 Carbon Steel
78 Plate for Boilers and Pressure Vessels.

76

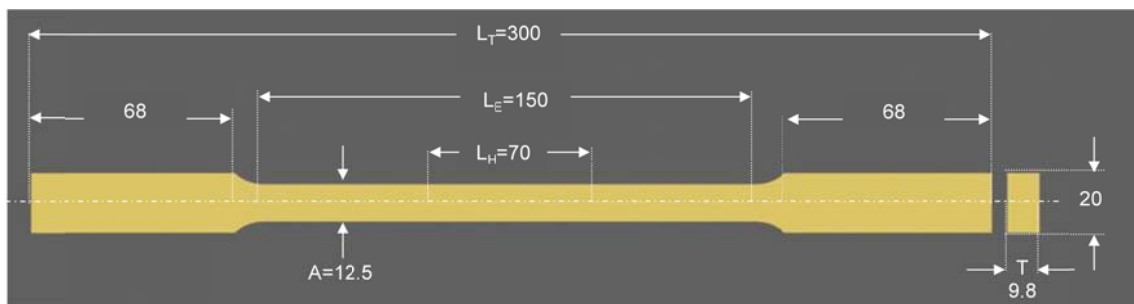
77 **Table 1. Composition of Carbon steel A516 Grade 70 [12].**

Composition	Content (% wt.)
Fe (Iron)	Base Element (>98)
C (Carbon)	0.27
Mn (Manganese)	0.79-1.3
S (Sulphur)	0.025
Si (Silicon)	0.025
Mechanical properties	
Ultimate tensile strength (UTS)	485 – 620 MPa
Yield Strength	260 MPa (minimum value)
Elongation	15% (minimum value)

78

81 Specimens for mechanical testing were machined from the original plate by laser cutting. The
82 size of the specimens was calculated following the standard from the plate thickness [11].
83 Dimensions (in millimetres) and design of the specimens are shown in Figure 1.

82



83

84 **Figure 1 - Dimensions of the specimens machined from A516Gr70 plate [11].**

85

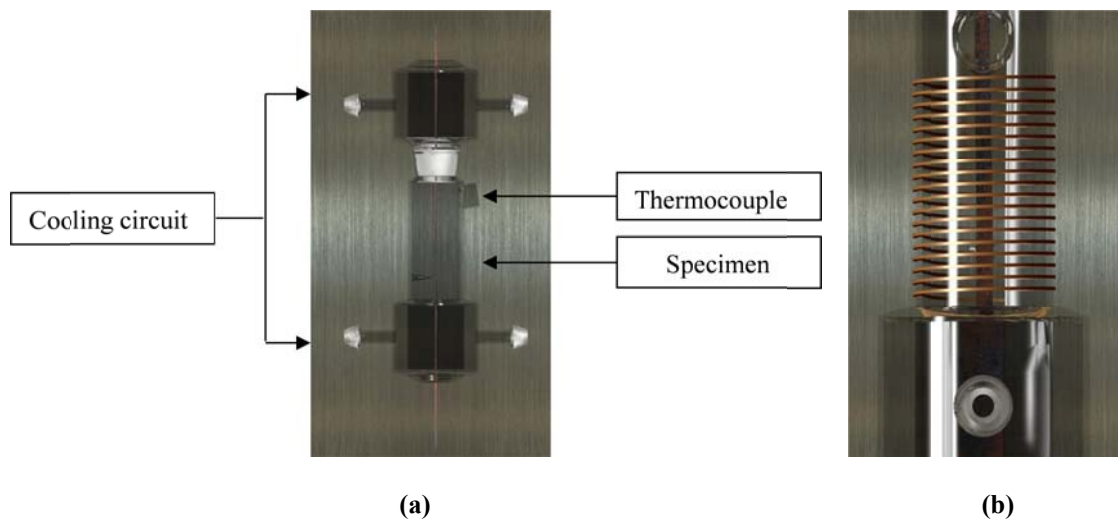
86

2.2. Experimental set up

91 A small furnace was designed and built at University of Barcelona to perform the tests at the
92 desired temperature (in this case 380 °C), having the specimen in contact with nitrate molten
93 salts during the mechanical testing. The mixture selected is the so-called *Solar salt* reported in
94 the literature with a composition 60:40 NaNO₃ and KNO₃ by weight, close to the eutectic
95 composition.

98 The cylindrical device was made of quartz, and its size allows testing the central part of the
99 samples. A specific opening was designed to introduce a thermocouple to monitor the molten
1.00 salts temperature as shows the scheme of Figure 2.(a). The top and the bottom of the device are
1.01 designed so that a refrigeration circuit using water as heat transfer fluid may be coupled, to
1.02 prevent molten salts leakage. Furthermore, it also has the central part with a reduced section in
1.03 which an electrical resistance was coiled around, see Figure 2.(b), and then fully thermally
1.04 insulated, see Figure 3.

99

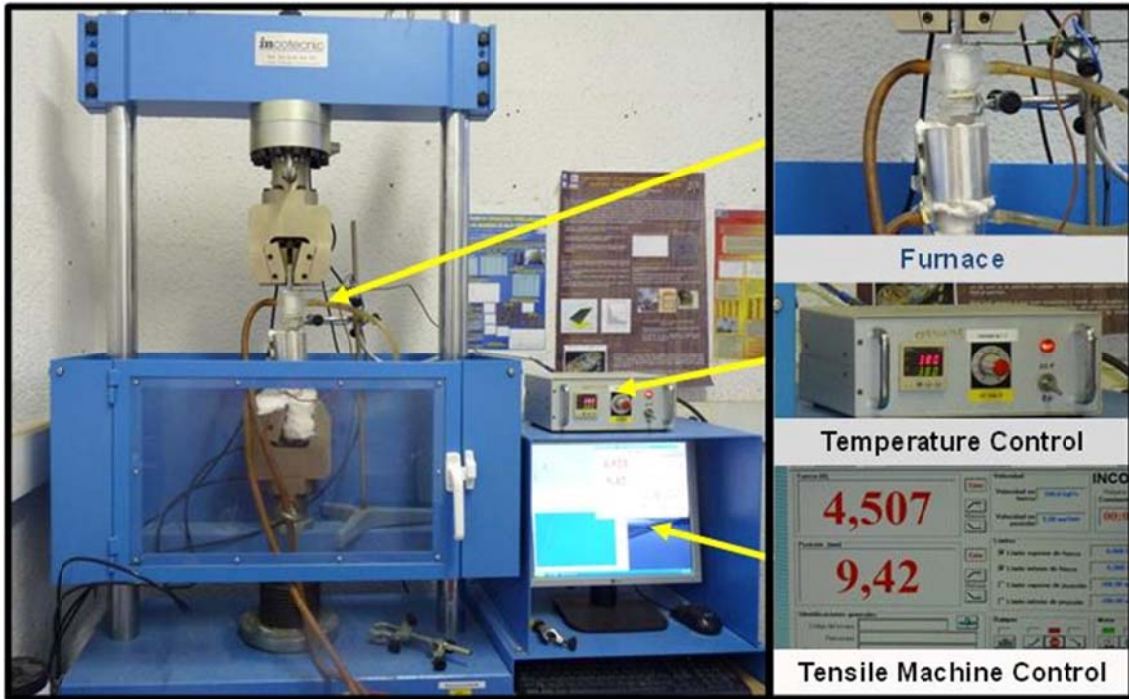


1.00

Figure 2. (a) Small furnace devise; (b) Heating source

103 The insulated system keeping the length of reduced section of the specimen in contact with
104 molten salts is presented in the upper right part of Figure 3. The sample is then fixed through the
105 jaws to the mechanical testing machine Incotecnic MUTC-200.

104



105

106

Figure 3 - Picture of the experimental set-up

107

109 In order to evaluate the effect of temperature on the mechanical behaviour, three different
 110 experiments were performed.

113 First experiment: the material under study was first tested at room temperature. The tensile test
 114 was carried out at a loading rate of $5 \text{ mm} \cdot \text{min}^{-1}$ until failure. Then, the conventional diagrams
 115 plotting stress (σ) vs. % strain ($\epsilon\%$), where stress and strain are defined with Eq. 1 and Eq. 2,
 116 were calculated:

114

$$\sigma \text{ (MPa)} = \frac{F \text{ (N)}}{S \text{ (mm}^2\text{)}} \quad \text{Eq. 1}$$

$$\% \epsilon = \frac{\Delta l \text{ (mm)}}{l \text{ (mm)}} \times 100 \quad \text{Eq. 2}$$

115

118 where F is the applied force (in N) and S is the area perpendicular to the application of force, in
 119 the case of the specimens tested it is 122.5 mm^2 and to calculate it, l is fixed to 205 mm , being
 120 the distance between jaws.

120 The yield strength obtained from the conventional diagram was used as a reference yield
 121 strength to perform the next mechanical tests at higher temperature.

120 Second experiment: the effect of the temperature on the mechanical properties was tested using
121 the device described previously, having the central part with reduced section in contact with the
122 molten salts at 380 °C. Notice that the sample was in contact with the molten salts not only
123 during the mechanical-test but also during the heating processes (the heating rate applied was 5
124 °C·min⁻¹). Once the temperature of the salts reached 380 °C, the sample was left five more
125 minutes to homogenize the temperature of the specimen. Afterwards, the specimen was tested at
126 380 °C under a loading rate of 5 mm·min⁻¹ until the sample fractured in order to observe if the
127 temperature affected the mechanical properties. It is important to remark that the main objective
128 of performing these tensile strength tests (out of standards) is to determine the temperature
129 effect instead of determining high precision values for mechanical properties. Even though, the
130 obtained results can be used to perform a comparison in order to differentiate mechanical
131 behaviours, being this comparison semi-quantitative.

132 Third experiment: as seen so far, the mechanical behaviour of the steel tested change when
133 working at high temperature. In order to determine a possible variation of the properties under
134 working conditions (load, temperature, and contact with molten salts) a specific experiment was
135 designed. It consists in applying a load (39200 N) and keeping the specimen contact with
136 molten salts during 7 days under a constant elongation (4.79 mm): this test is known as creep-
137 test in materials engineering field.

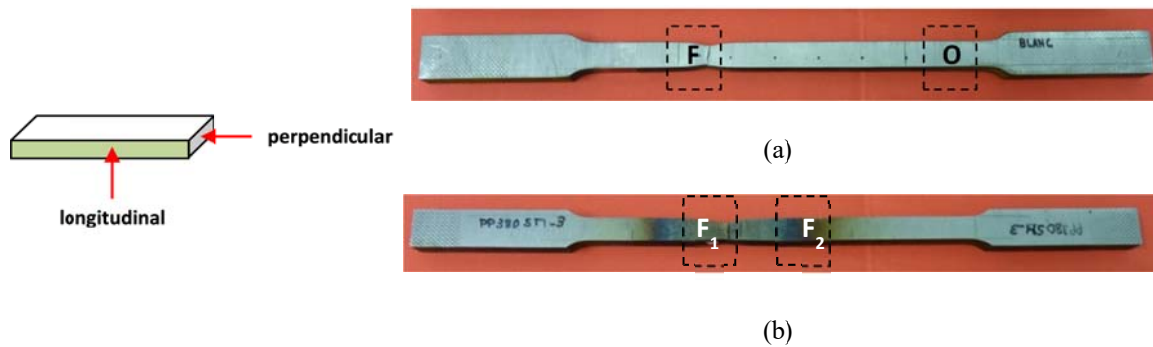
138 The experimental procedure consisted on applying an initial load. This load has to be below the
139 one obtained by measuring yield strength of a A516Gr70 steel sample immersed in molten salts
140 at 380 °C (second experiment).. Therefore, regarding the load a safety factor of 1.25 was used to
141 perform thermo-mechanical experiments, which is commonly used for exceptionally reliable
142 materials used under controllable conditions [9]. After the creep-test, a tensile strength test was
143 performed at 380 °C (inside the device) under a loading rate of 5 mm·min⁻¹ until the sample
144 fracture too.

145

146 **2.3. Metallographic study**

147 After the failure, different zones of the tested specimen at 380 °C were cut and prepared for the
148 metallographic study. Sample preparation follows the ASTM standard [13] for steel samples,
149 and the etching agent used to reveal the microstructure was Nital (98%v/v ethanol, 2%v/v
150 HNO₃).

151 For each sample, the microstructure was observed in two different zones: zone F is the failure
152 zone and zone O is a zone of the reduced section far from the failure. Moreover, the
153 microstructure was observed from both applied force directions, longitudinal and perpendicular
154 to the application of stress as Figure 4 shows.



158 **Figure 4 - Zones where the metallographic study was performed with (a) samples measured under**
 159 **380 °C and (b) sample tested under 380 °C after 7 days**

160 Notice that the temperature of F, F1 and F2 zones were at 380 °C because these zones are inside
 161 the furnace and 25 °C is the temperature outside the furnace (O zone).

161

162 3. Results and discussion

163 3.1. Mechanical testing

175 Mechanical properties obtained from the tensile strength test under room temperature conditions
 176 are shown in Figure 5 (blue line). The yield strength obtained ($\sigma_{0,2}$) is ~400 MPa and the
 177 elongation 17%. Comparing these results with the specifications for a steel of this grade, the
 178 yield obtained in the test performed is well above the minimum specified for this material (260
 179 MPa), while the measured elongation is slightly higher than the minimum specified (15%). In
 180 addition, tensile strength test results for the sample tested at 380 °C in contact during 5 minutes
 181 with molten salts are also shown in Figure 5 (orange line). In this case, the yield strength ($\sigma_{0,2}$)
 182 is about 340 MPa and the strain percentage 13%, showing lower plastic deformation. To
 183 calculate the strain the initial length used was $L_0 = 205$ mm in order to use the same one than in
 184 the test before (ambient temperature). In this test, the reduction of the Young Modulus with
 185 temperature is also noticeable. The change of this and other properties is described following
 186 the equation [14]:

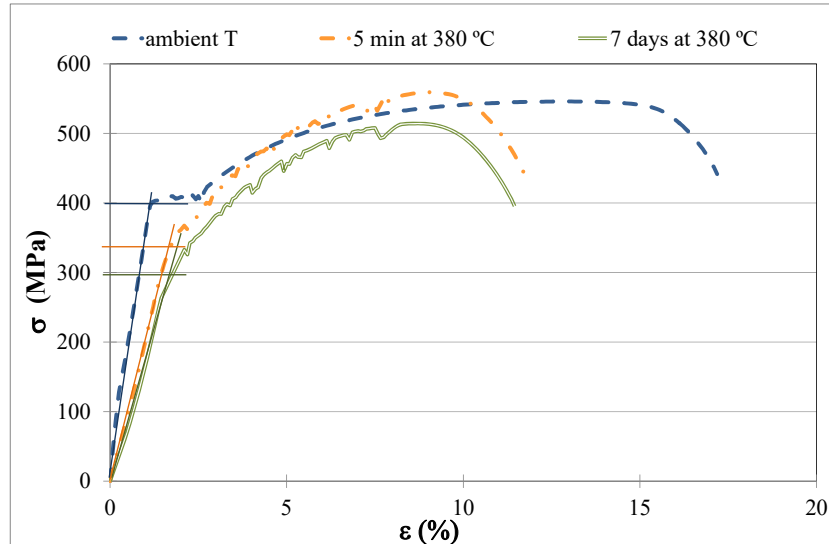
176

$$177 \quad P \approx P_0 \left(1 + \beta \frac{T}{T_m} \right) \quad \text{Eq. 3}$$

178

180 where P is the property at a given temperature T (K), P_0 is the property at 25°C, β is a constant
 181 ($\beta \approx -0.5$ for metals), and T_m is the melting temperature (K). This equation predicts a reduction

180 of the Young Modulus of around 19% that should be also considered during the mechanical
 181 design. But in the experiments presented, 40% reduction of Young Modulus was calculated
 182 from the obtained curves. A more accurate Young Modulus values could be expected with the
 183 use of an extensometer, but this device is not available.



184

185 **Figure 5 - Conventional diagram of A516GR70 specimen tested at room temperature (blue line),**
 186 **tested at 380°C (orange line), and tested at 380 °C after 7 days creep-test (green line)**

187

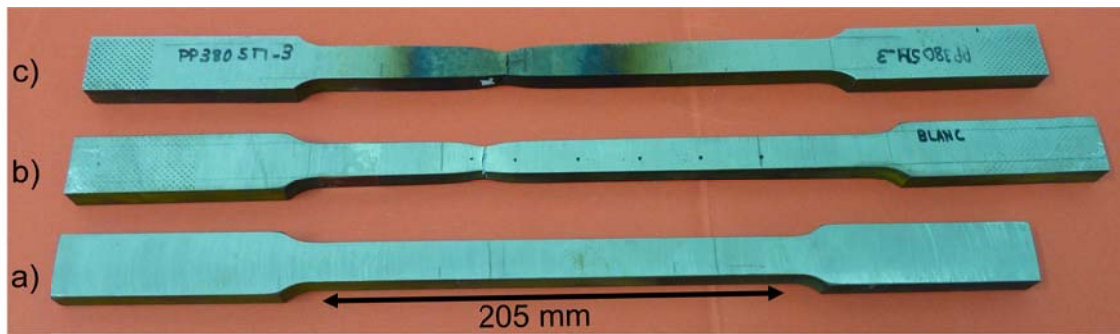
188 The part of the specimen in contact with the molten salts at 380 °C begins to deform plastically
 189 at a lower load, while the rest of the specimen is at a lower temperature, still working in the
 190 elastic range. This assumption is verified by measuring the dimensions of the specimens after
 191 the test.

192 In the sample tested at 380 °C, dimensions change only in the region in contact with molten
 193 salts, whereas in the specimen tested at room temperature, all the central part with a reduced
 194 section changed its dimensions.

195 In the sample tested at room temperature (blue line), when the stress is increased, the strain is
 196 slightly increased (steep slope) until a critical stress value (yield strength). After that, low
 197 increments in load produced high elongation (yield zone). The behaviour shown in this area is
 198 due to oblique surface slides caused by shear stress (Luders bands). However, when the
 199 material is tested under 380 °C, the yield zone disappears because the temperature disables
 200 sliding surface mechanisms [15] or the temperature decreases the yield strength.

201 Finally, Figure 6 shows the specimens that have undergone necking in the area of rupture,
 202 showing a ductile failure with plastic deformation in both cases (room temperature and under
 203 380 °C).

205



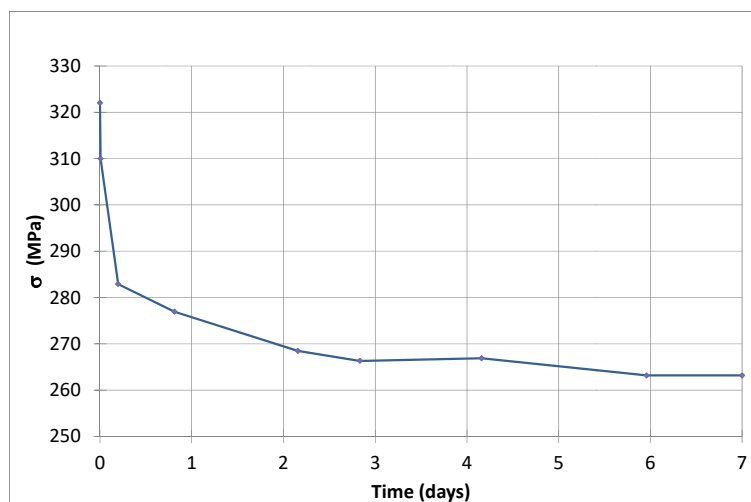
206

208 **Figure 6 - Specimen of A516GR70 (a) before the tensile strength test, (b) after the tensile test at**
209 **room temperature, (c) after the tensile test at 380 °C**

209

215 In order to evaluate the performance under operational conditions, the sample was tested at 380
216 °C in contact with molten salts during 7 days by applying an initial load of 320 MPa (below the
217 yield strength measured at 380 °C). The elongation produced by applying this load was 4.79
218 mm. Then, this elongation was kept constant during the 7 days of test and load was registered
219 over time. Notice that the stress required to keep a constant elongation decreases over time to an
220 asymptotic value (approximately 265 MPa) due to stress relaxation, as Figure 7 shows.

216



217

218 **Figure 7 - Change in the stress needed to keep a constant elongation of 4.79 mm at 380 °C**

219

223 Once 7 days have elapsed, a new tensile test was performed on the sample and the conventional
224 diagram obtained is also shown in Figure 5. Thereby, the yield strength is less than 300 MPa,
225 about 40 MPa lower than that obtained when the specimen had only been 5 minutes at 380 °C
226 (Figure 6). The elongation at fracture was very similar while the measured yield strength was

226 higher than the 260 MPa accepted as minimum value in the standard. The material anneals from
227 the beginning and this annealing continues during this period of 7 days of performance under
228 load, at 380 °C and in contact with molten salts.

230 Therefore, when a creep test is performed (7 days, 380 °C, 320 MPa) the sample is plastically
231 deformed, and hence, in a posterior tensile strength test the deformation mechanisms are
232 disabled due to the previous plastic deformation [14] and the ultimate tensile strength also
233 decreased.

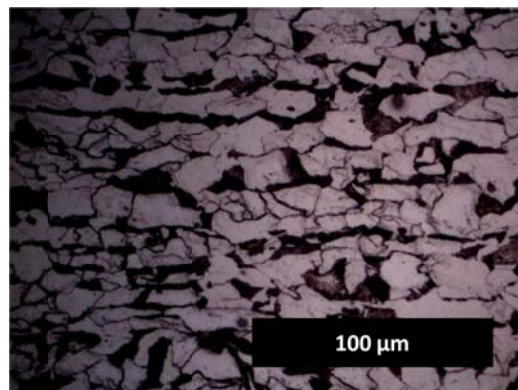
231

232 3.2. Metallographic study

234 Since there were differences in the mechanical response upon the testing conditions, the study
235 of the microstructure prior and after each step was done to complement the obtained results.

236 The longitudinal section of the initial microstructure at 50x magnification is shown in Figure 8.
237 The grains are equiaxially oriented following the shaping direction of the sheet.

237



238

239 **Figure 8- Initial longitudinal microstructure of A516Gr70 carbon steel sample**

240

245 The microstructure of samples tested at room temperature is shown in Figure 9 applying 50x
246 magnification. Figure 9.(a) and 9.(b) show a microstructure with oriented equiaxial grains, due
247 to the shaping of the sheet. In the image of the longitudinal failure zone shown in Figure 10.(c),
248 the grains deformed in the direction of application of force during the tensile test are observed.
249 Moreover, notice that the grains became smaller due to the force applied, as Figure 9.(d) shows.

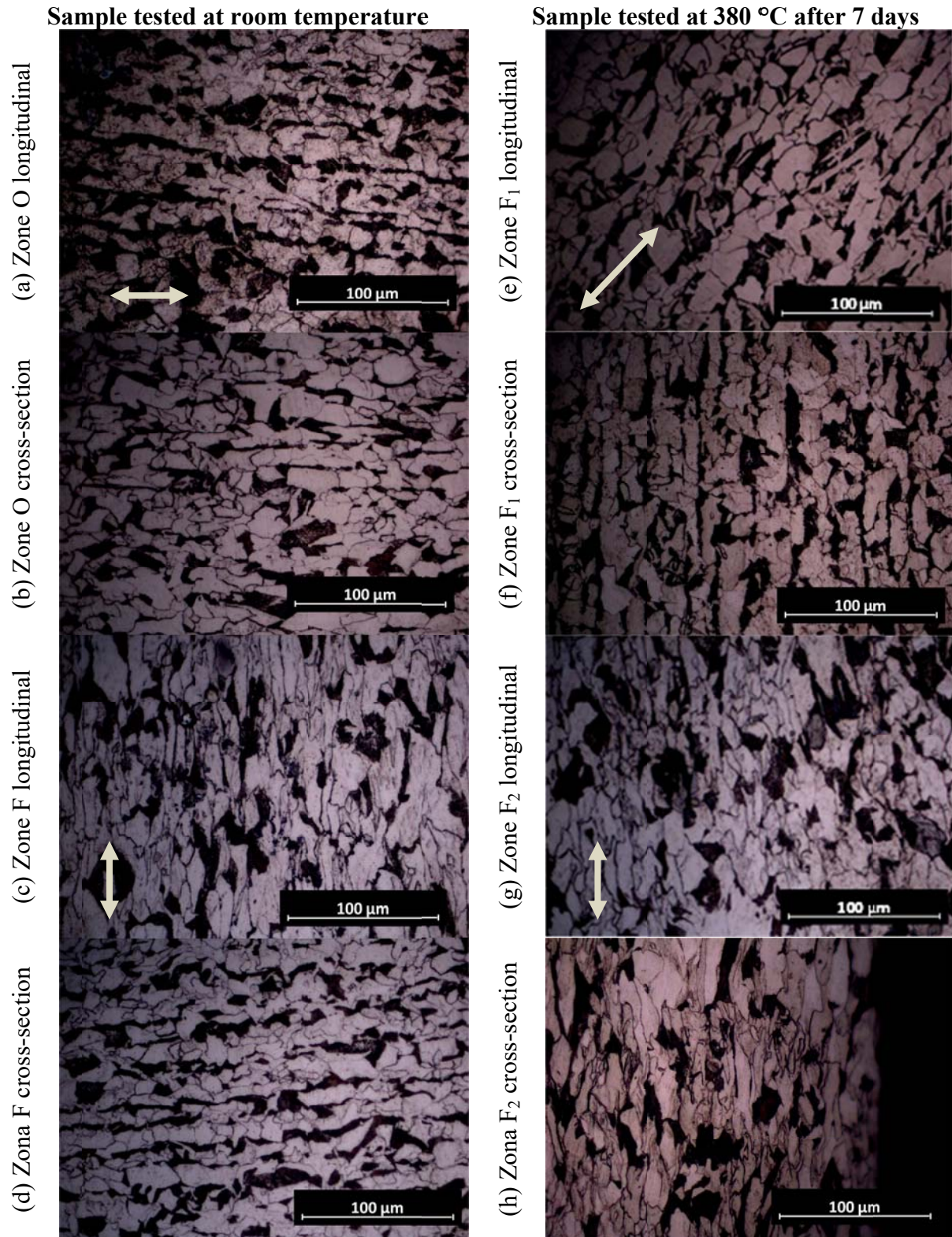
249 On the other hand, Figure 9.(e) and Figure 9.(f) show the areas where the microstructure and the
250 longitudinal and cross direction of samples tested at 380 °C during 7 days can be seen. The
251 longitudinal failure zone (F_1) observed in Figure 9.(e) shows that the grains are deformed in the
252 direction of the applied force (\uparrow). Moreover, the cross-section of the broken zone (F_1) is shown

249 in Figure 9.(f) where the grains are highly deformed losing their initial form. On the other hand,
250 the grains are slightly affected and preserve almost the same form as the original one in the
251 longitudinal section outside of the failure zone (F_2), as shown in Figure 9.(g).

252 Even though the operational conditions are reported as corrosives, corrosion evidences appear at
253 longer exposure times and there is no evidence of intergranular corrosion in the metallographic
254 analysis of samples under load at 380 °C, in contact with molten salts for 7 days.

255 The reduction of yield strength and elongation is attributed to the annealing of the sample and
256 this fact is corroborated with the metallographic study as shown in the deformation in
257 concordance with the direction (see Figure 9).

258



267 Figure 9- Microstructure of the samples tested under the following conditions: (a) Longitudinal section outside
 268 of the broken part of the samples tested at room temperature; (b) Cross-section outside of the broken part of
 269 the samples tested at room temperature; (c) Longitudinal section outside of the broken part of the samples
 270 tested at room temperature; (d) Cross-section outside of the broken part of the samples tested at room
 271 temperature; (e) Longitudinal section in the broken part of the samples treated at 380 °C during 7 days; (f)
 272 Cross-section in the broken part of the samples treated at 380 °C during 7 days; (g) Longitudinal section
 273 outside of the broken part of the samples treated at 380 °C during 7 days; (h) Cross-section section outside of
 274 the broken part of the samples treated at 380 °C during 7 days

268 * Notice that arrows indicate the direction load applied during the tensile strength test

4. Conclusions

An experimental setup to perform the mechanical testing of steel A516Gr70 under operational conditions at 380 °C in contact with molten salts was designed and built.

Mechanical testing under operational conditions confirmed the reduction of yield strength and Young Modulus as well as the elongation compared with testing at room temperature. The measured yield strength is above the limit defined in the ASTM standard.

A seven days creep-test experiment maintaining the sample under working conditions and a load below the yield strength was performed. Changes in mechanical properties after the creep-test are confirmed: the reduction of yield strength and elongation are attributed to the annealing of the sample and this fact is corroborated with the metallographic study carried out.

Acknowledgements

The research leading to these results has received funding from Spanish government (Fondo tecnológico IDI-20090393, ConSOLida CENIT 2008-1005). The work is partially funded by the Spanish government (ENE2011-28269-C03-02, ENE2011-22722, ENE2015-64117-C5-1-R, and ENE2015-64117-C5-2-R). The research leading to these results has received funding from the European Union's Seventh Framework Programme (FP7/2007-2013) under grant agreement n° PIRSES-GA-2013-610692 (INNOSTORAGE) and from the European Union's Horizon 2020 research and innovation programme under grant agreement No 657466 (INPATH-TES). The authors would like to thank the Catalan Government for the quality accreditation given to their research groups GREA (2014 SGR 123) and research group DIOPMA (2014 SGR 1543). Dr. Camila Barreneche would like to thank Ministerio de Economía y Competitividad de España for Grant Juan de la Cierva FJCI-2014-22886.

References

1. V. Devabhaktuni, M. Alam, Shekara Sreenadh Reddy Depuru, S. Green II, R.C. Nims, D., C. Near. Solar energy trends and enabling technologies. *Renew Sustain Energy Rev*, 19 (2013), pp. 555–564.
2. Chu Y. Review and comparison of different solar energy technologies. *Research Associate Global Energy Network Institute (GENI)*, vol. 619; 2011, p. 595-0139.

- 301 3. U.S. Department of Energy. Integrated solar thermochemical reaction system. Available
302 from: [http://energy.gov/eere/sunshot/project-profile-integrated-solar-thermochemical-
304 reaction-system](http://energy.gov/eere/sunshot/project-profile-integrated-solar-thermochemical-
303 reaction-system) (retrieved 01.12.2016)
- 304 4. Jibrán Khan, Mudassar H. Arsalan. Solar power technologies for sustainable electricity
305 generation – A review. *Renewable and Sustainable Energy Reviews* 55 (2016) 414–
306 425.
- 307 5. U. Desideri, F. Zepparelli, V. Morettini, E. Garroni. Comparative analysis of
308 concentrating solar power and photovoltaic technologies: technical and environmental
309 evaluations. *Appl Energy*, 102 (2013), pp. 765–784
- 310 6. Ming Liu, Wasim Saman, Frank Bruno. Review on storage materials and thermal
311 performance enhancement techniques for high temperature phase change thermal
312 storage Systems. *Renewable and Sustainable Energy Reviews* 16 (2012) 2118–2132
- 313 7. Sarada Kuravi, Jamie Trahan, D. Yogi Goswami, Muhammad M. Rahman, Elias K.
314 Stefanakos. Thermal energy storage technologies and systems for concentrating solar
315 power plants. *Progress in Energy and Combustion Science* Volume 39, Issue 4, August
316 2013, Pages 285–319
- 317 8. Prieto C, Fernández AI, Cabeza LF. Molten salt facilities, lessons learnt at pilot plant
318 scale to guarantee commercial plants. Plant description and start-up recommendations.
319 Accepted for publication in *Renewable Energy*
- 320 9. Ugural, A. C. *Mechanical design. An integrated approach*. Mac Graw Hill, 2004 (p52)
321 USA. ISBN 0-07-242155-X
- 322 10. Prieto C; Fernández, A.I.; Cabeza, L.F. Molten salt facilities, lessons learnt at pilot plant
323 scale to guarantee commercial plants. Part 1 – Plant description and start-up
324 recommendations (paper submitted to *Renewable Energy*).
- 325 11. ASTM Standard: ASTM E8 / E8M - 15a. Standard Test Methods for Tension Testing of
326 Metallic Materials
- 327 12. CES Selector Database. Granta Design, Cambridge 2012.
- 328 13. ASM International. *ASM Handbook: Metallography and microstructures*, vol 9. UK.
329 ISBN: 0-87170-706-3. 2004.
- 330 14. Ashby MF, Shercliff H, Cebon D. *Materials: Engineering, Science, Processing and
331 Design*. Butterworth-Heinemann, 2007, ISBN 9870750683913.
- 332 15. Beer FP, Russell Johnston Jr. E, DeWolf JT, Mazurek DF. *Mechanics of materials*. Mc
333 Graw Hill, 7th edition, 2015, 978-0073398235.